Supporting Information

Simultaneous water and electricity harvesting from low-grade heat by coupling membrane distillation system and electrokinetic system

Lu Huang[1,2†], An He[1†], Mengyu Miao[1†], Junxian Pei[3], Tong Liu[1,2*], Xiaojuan Lei[4], Kunpeng Shan[1], Shuting Lei[1], Yipu Wang[1], Pinxuan He[1], Quan Feng[1], Zhifeng Huang[1*], Xuejiao Hu[1] and Haifeng Jiang[1*]

[1]MOE Key Laboratory of Hydraulic Machinery Transients, School of Power and Mechanical Engineering, Wuhan University, Wuhan, Hubei, 430072, China

[2] School of Mechanical & Electrical Engineering, Wuhan Institute of Technology, Wuhan, Hubei, 430205, China

[3] College of Water Resource & Hydropower, Sichuan University, Chengdu, 610065, China

[4] College of Food Science, Southwest University, Chongqing, 400715, China

[†]These authors contributed equally to this work.

*Corresponding authors. E-mail addresses: liu_tong@whu.edu.cn (T. Liu), zfhuang@whu.edu.cn (Z. Huang), hfjiang@whu.edu.cn (H. Jiang).

Table of contents

SI-1 Schematic diagram and photograph of the EPG device

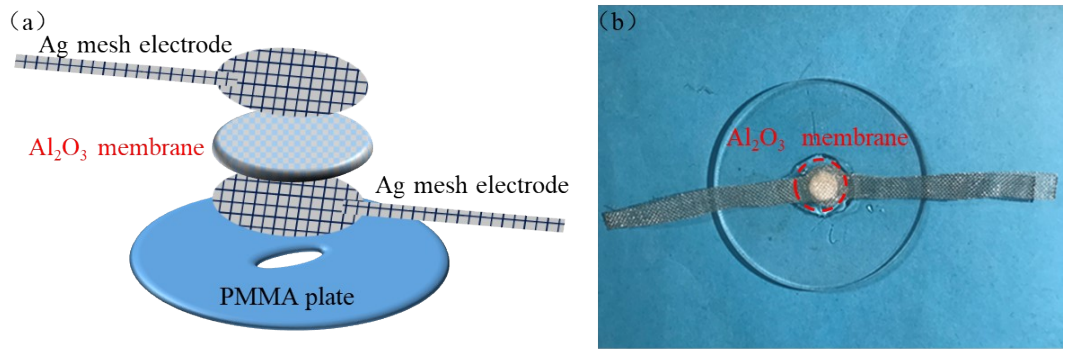

Fig. S1 (a) Schematic diagram of the assembly of the EPG device; (b) Physical drawing of the EPG device.

SI-2 The schematic diagram of the experimental measurement system

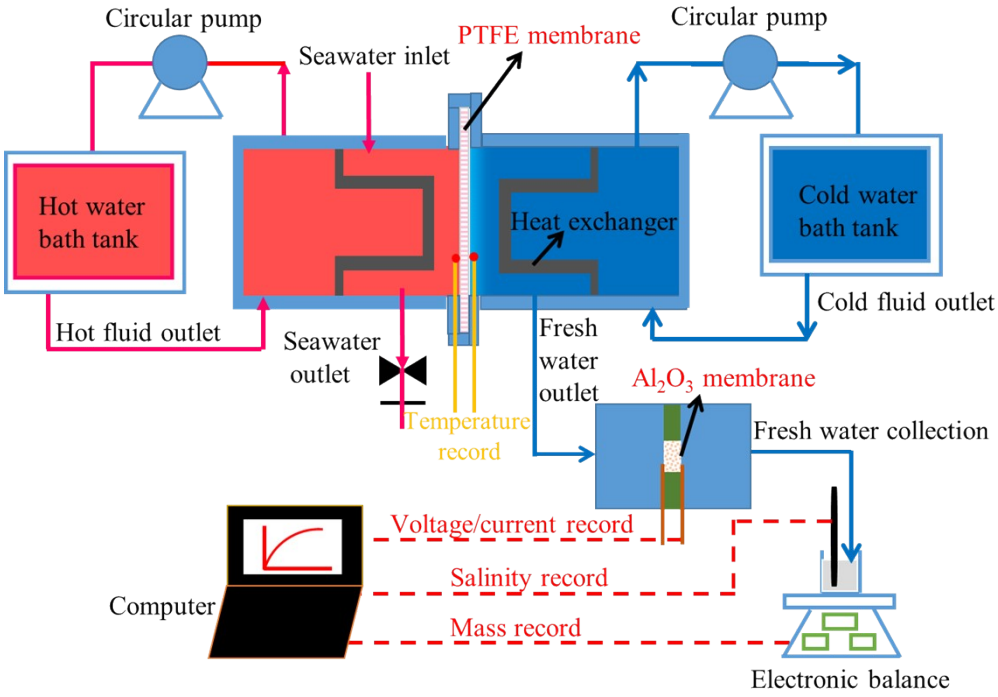

Fig. S2 The schematic diagram of the experimental measurement system, including: (1) a computer for data record and storage, (2) two type K thermocouples for temperature collection, (3) an electronic balance for weight change record, (4) a source meter for potential/current record, (5) a conductivity meter for desalted water quality.

SI-3 The contact angle measurement of Al_2O_3 membrane

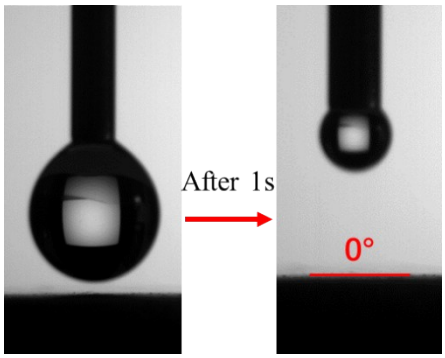

Fig. S3 The contact angle measurement of Al_2O_3 membrane.

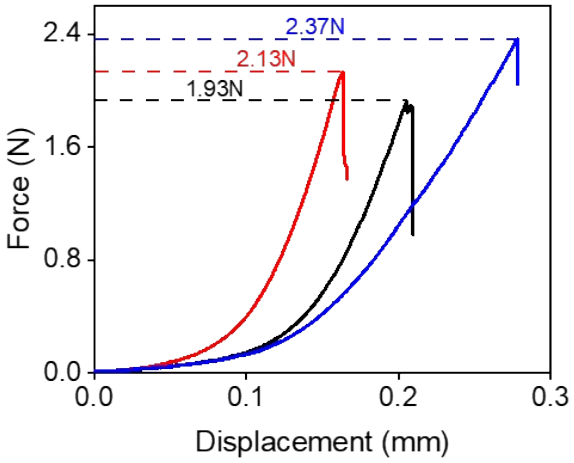

SI-4 Pressure-displacement curves of three paralleled Al_2O_3 membrane samples

Fig. S4 Pressure-displacement curves of three parallel Al_2O_3 membrane samples

SI-5 The relationship between output voltage and input pressure over time of the EPG device

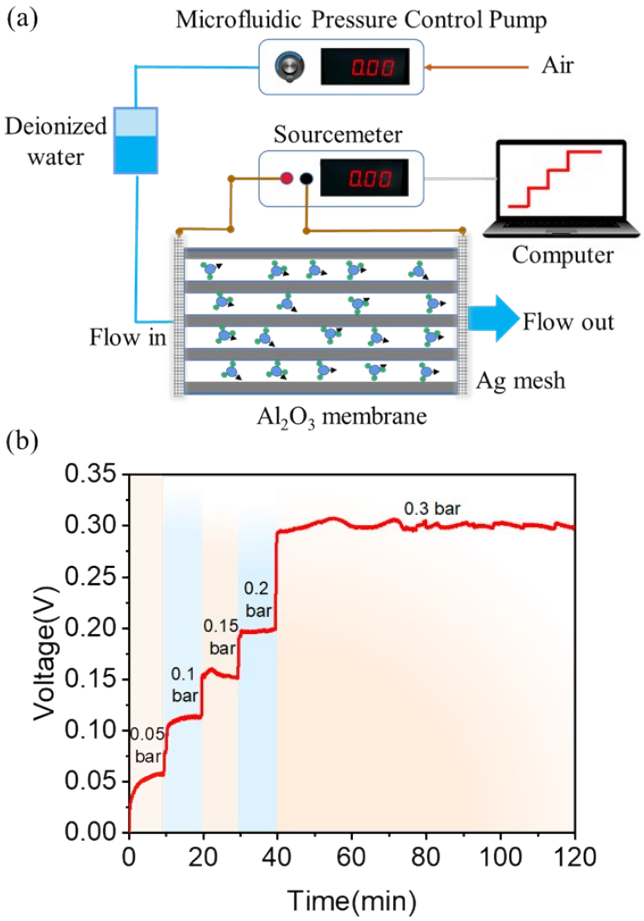

Fig. S5 (a) A diagram of the self-made test system; (b) The relationship between output voltage and input pressure over time.

SI-6 The energy exchange efficiency of the EPG device

The EPG device's efficiency is an important indicator reflecting the utilization rate of the hydraulic pressure energy, which can be calculated as:

$$\eta = \frac{P_{out}}{P_{in}} = \frac{P_{out}}{\Delta P Q} \tag{S-0}$$

where P_{out} (W m^{-2}) is the maximum output power density of the EPG device under under different temperature differences, calculated from the I-V curve. ΔP (Pa) is hydraulic pressure difference on both sides of Al_2O_3 membrane under different temperature differences, calibrated by the pressure gauge. Q (m s^{-1}) is the volume flow under different temperature differences, obtained by dividing the mass flow by the water density.

In our experiments, the maximum output power density of the EPG system under the temperature difference of 20 °C, 30 °C and 40 °C is approximately 27 μW m^{-2}, 68 μW m^{-2}, and 147 μW m^{-2}, respectively. The corresponding hydraulic pressure difference on both sides of Al_2O_3 membrane is ~2.4 KPa, ~3.5 KPa, ~5.2 KPa under the temperature difference of 20 °C, 30 °C and 40 °C. The corresponding volume flow under the temperature difference of 20 °C, 30 °C and 40 °C is 1.36×10^{-6} m s^{-1}, 2.72×10^{-6} m s^{-1}, and 3.72×10^{-6} m s^{-1}, respectively. According to formula S-0, it can be calculated that the corresponding efficiency of the EPG device is 0.83%, 0.71% and 0.76% under the temperature difference of 20 °C, 30 °C and 40 °C.

SI-7 Dynamic response characteristics of the EPG device

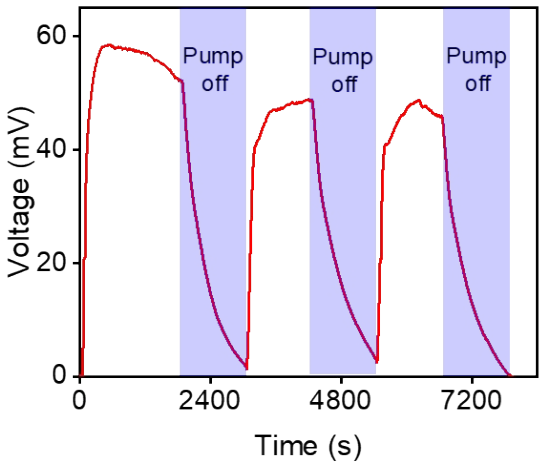

Fig. S6 The influence of periodically switching circulating pump on open circuit voltage of the EPG device.

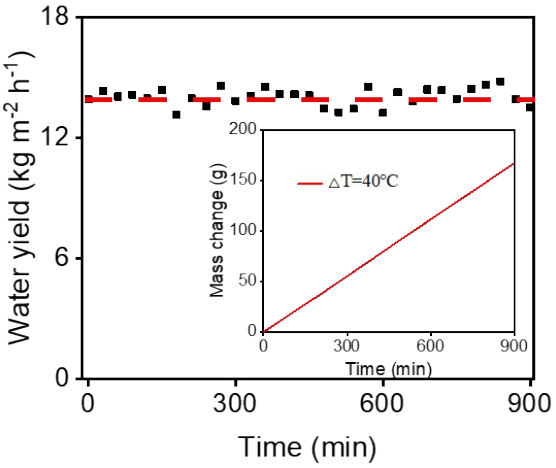

SI-8 The water yield varies with time within 15 hours

Fig. S7 The water yield varies with time within 15 hours and the inset is the mass change over time at a temperature difference of 40℃

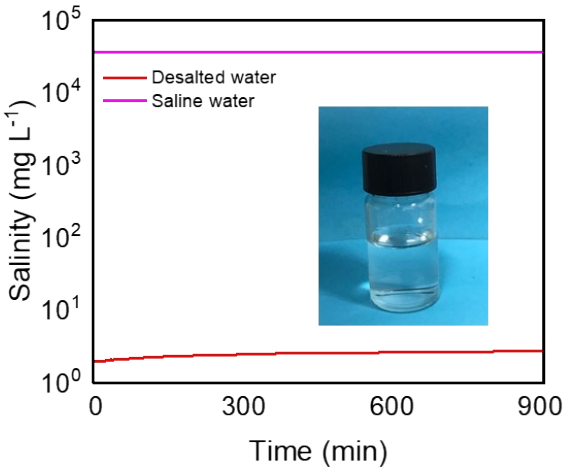

SI-9 The salinity of desalinated water varies with time

Fig. S8 The salinity of desalinated water varies with time.

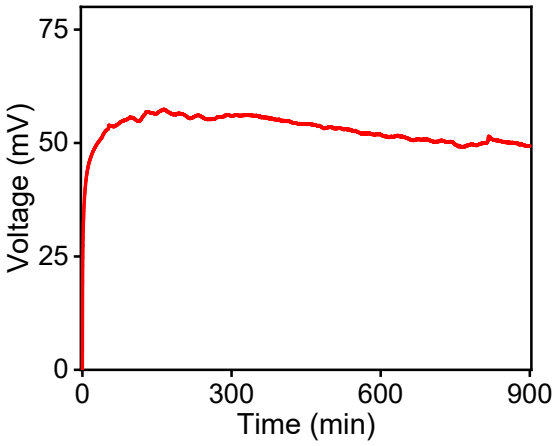

SI-10 Open circuit voltage as a function of time within 15 hours

Fig. S9 Open circuit voltage as a function of time within 15 hours.

SI-11 A steady-state heat transfer model of the MD-EPG system

Fig. 4a shows the steady-state energy and mass transfer equilibrium diagram of the MD-EPG system. In order to more specifically analyze the internal heat and mass transfer and energy conversion process of the tandem system, we have made the following assumptions for the model:

1. The model is a steady-state model. Heat and mass are dominated by one-dimensional transfer;

2. Suppose the heat source on the high temperature side of the system comes from low-grade thermal energy in the environment;

3. Ignore the temperature polarization effect, that is, the temperature on both sides of the hydrophobic membrane remains unchanged;

4. The influence of the change in salt concentration caused by the evaporation of salt water in the system on water evaporation is negligible;

5. Regardless of the hydraulic pressure breaking through the liquid entry pressure of the hydrophobic membrane, the MD process becomes invalid.

Based on the theoretical model, the corresponding mathematical equations of the heat and mass transfer process and the relationship of energy and mass conservation are obtained. The input energy of the entire system (Q_{in}) is the sum of the latent heat taken away by water evaporation through the hydrophobic membrane (Q_{eva}) and the heat conducted through the solid part of the PTFE membrane (Q_{con}). According to the law of conservation of energy, the energy conservation relationship of the MD unit can be described as :[1]

$$Q_{in} = Q_{con} + Q_{eva} \tag{S-1}$$

$$Q_{eva} = JH_v \tag{S-2}$$

$$Q_{con} = \frac{k_{eff}}{l} * (T_e - T_c) \tag{S-3}$$

$$k_{eff} = k_{air}\varepsilon_m + k_{mem}(1 - \varepsilon_m) \tag{S-4}$$

$$H_v = 1.05 \times 10^{-7} T_e^4 - 4.17 \times 10^{-5} T_e^3 + 0.003 T_e^2 - 2.43 T_e + 2501.9 \times 10^3 \quad \text{(S-5)}$$

where T_e is the evaporation side temperature of the PTFE membrane, T_c is the condensation side temperature of the PTFE membrane (298.15 K), k_{eff} is the effective thermal conductivity of the hydrophobic PTFE membrane (W m^{-1} K^{-1}); k_{mem} and k_{air} are the thermal conductivity of PTFE membrane and air (W m^{-1} K^{-1}), which are 0.25 W m^{-1} K^{-1} and 0.028 W m^{-1} K^{-1}, respectively; ε_m is the porosity of the PTFE membrane (0.85, data from manufacturers), l is the thickness of the PTFE membrane ; J is the mass flux of water vapor across the membrane(kg m^{-2} s^{-1}), H_v is the latent heat of vaporization of water (J kg^{-1}).

The vapor flux through the hydrophobic PTFE membrane is:[2]

$$J = B_w(P_e - P_{c,h}) \quad \text{(S-6)}$$

where B_w is the vapor diffusion coefficient. Because the average free path of water vapor is equal to the pore size, the diffusion mode of water vapor through hydrophobic membrane is dominated by molecular diffusion and Knudsen diffusion. The calculation process is as follows: [3]

$$B_w = \frac{1}{\frac{1}{B_m} + \frac{1}{B_k}} \quad \text{(S-7)}$$

The coefficient B_m is used to describe the strength of molecular diffusion, and its expression is:

$$B_m = \frac{\varepsilon D M}{\tau L R T m/(P_0 - P_m)} \quad \text{(S-8)}$$

The coefficient B_k is used to describe Knudsen diffusion, and its expression is: [4]

$$B_k = \frac{2\varepsilon_m r M}{3\tau L R} * \sqrt{\frac{8R\pi M}{T_m}} \quad \text{(S-9)}$$

$$D = 1.894 \times 10^{-5} (T_m + 273.15)/P_0 \quad \text{(S-10)}$$

$$\tau = \frac{(2-\varepsilon)^2}{\varepsilon} \quad \text{(S-11)}$$

$$T_m = (T_e + T_m)/2 \quad \text{(S-12)}$$

where D is the diffusion coefficient of water vapor in the air; M is the molar mass of water (0.018 kg mol^{-1}); τ is the tortuosity of the PTFE membrane; r is the average radius of the pores of the PTFE membrane (0.5 μm); R is the gas constant (8.314 J K^{-1} mol^{-1}); T_m is the average temperature of the entire PTFE membrane; P_0 is the atmospheric pressure (101300 Pa).

The vapor pressure on the high temperature side (P_e) and (P_m) are calculated by Antoine equation under atmospheric pressure:[5, 6]

$$P_e = exp(23.1964 - 3816.44/(-46.13 + T_e + 273.15)) \quad \text{(S-13)}$$

$$P_m = exp(23.1964 - 3816.44/(-46.13 + T_m + 273.15)) \quad \text{(S-14)}$$

For the vapor pressure at the condensing side ($P_{c,h}$), the increase of hydraulic pressure in the condensing chamber will hinder the vapor transfer process across the hydrophobic PTFE membrane, which is manifested by the increase in the partial pressure of water vapor on the condensation side of the hydrophobic membrane. The partial vapor pressure on the condensation side of the PTFE membrane can be calculated by the Kelvin equation modified by the hydrostatic pressure:[7]

$$P_{c,h} = P_c e^{\frac{P_h V_m}{RT_c}} \quad \text{(S-15)}$$

where P_c is the corresponding partial pressure of water vapor at T_c temperature under atmospheric pressure, which is determined by the Antoine equation under atmospheric pressure. V_m is the molar volume of liquid water (18 cm^3 mol^{-1}). P_h is the hydraulic pressure in the confined space, and the corresponding value can be calculated using the flow resistance model; The flow resistance (R) of the Al_2O_3 membrane is calculated as follows:

$$R = \frac{\mu\delta}{KA} \quad \text{(S-16)}$$

where μ is the dynamic viscosity of water at 25 °C, the value is 0.8937×10^{-3} Pa · s, δ is the thickness of the Al_2O_3 membrane (m), K is the permeability of the Al_2O_3 membrane (m^2), which reflects the difficulty of water flowing through its internal pores. The theoretical calculation value of K in this section is set to 2×10^{-17}. A is the area of

Al_2O_3 membrane (m^2).

According to the flow resistance of the Al_2O_3 membrane and the volume flow through the membrane, the hydraulic pressure difference (ΔP) in the enclosed space can be obtained, which is the hydraulic pressure P_h in the enclosed space, so the following expression is obtained:

$$P_h = \Delta P = JR = J\frac{A_1\mu\delta}{KA\rho} \tag{S-17}$$

Where ρ is the density of desalinated water (1000 kg m^{-3}), A_1 is the area of PTFE hydrophobic membrane (m^2).

According to the theoretical calculation results of hydraulic pressure difference (ΔP) on both sides of Al_2O_3 membrane and vapor flux (J) through the membrane under different transmembrane temperature difference, the maximum volume work output of alumina microporous membrane can be determined. The volume work calculation formula of the system is as follows: [8]

$$W = J\frac{\Delta P}{\rho} \tag{S-18}$$

In order to judge the heat-work conversion performance of the system more clearly, we use the relative Carnot cycle efficiency of the system to evaluate the performance of converting solar thermal energy into fluid mechanical energy. The relative Carnot cycle efficiency (η) of the system is calculated as follows: [8]

$$\eta = \frac{W}{\eta_c Q_{in}} \tag{S-19}$$

$$\eta_c = 1 - \frac{T_c}{T_e} \tag{S-20}$$

where Q_{in} is the input energy of the entire system, η_c is the Carnot cycle efficiency of the system.

References

1. M. Rahimi, A. P. Straub, F. Zhang, X. Zhu, M. Elimelech, C. A. Gorski and B. E. Logan, *Energy Environ. Sci.*, 2018, **11**, 276-285.

193 2. F. Mahmoudi, A. Date and A. Akbarzadeh, *J. Membrane Sci.*, 2019, **572**, 230-245.
194 3. M. Khayet. *Adv. Colloid Interface Sci.*, 2011, **164**, 56-88.
195 4. W. Kast, C. R. Hohenthanner, *Int. J. Heat Mass Transfer*, 2000, **43**, 807-823.
196 5. L. Huang, H. Jiang, Y. Wang, Z. Ouyang, W. Wang, B. Yang, H. Liu and X. Hu,
197 *Desalination*, 2020, **477**, 114260.
198 6. L. Huang, Y. Wang, R. He, X. Kong, S. Lei, Y. Liu, B. Wang, H. Jiang, H. Liu, K.
199 Liu and X. Hu, *Desalination*, 2020, **488**, 114533.
200 7. A. P. Straub, N. Y. Yip, S. Lin, J. Lee and M. Elimelech, *Nat. Energy*, 2016, **1**, 16090.
201 8. A. P. Straub and M. Elimelech, *Environ. Sci. Technol.*, 2017, **51**, 12925-12937.
202